International Journal of Science and Research (IJSR)
ISSN (Online): 2319-7064
Index Copernicus Value (2013): 6.14 | Impact Factor (2013): 4.438

Effect of Partial Shrouds on the Performance and Flow Field of a Low Speed Centrifugal Compressor

S. M. Swamy[1], V. Pandurangadu[2], N. Sitaram[3]

[1]G. Narayanamma Institute of Technology and Sciences, Shaikpet, Hyderabad, India

[2]J. N. T. U., College of Engineering Anantapur, A. P, India

[3]Department of Mechanical Engineering, Indian Institute of Technology, Madras, India

Abstract: ***The performance of a centrifugal compressor without and with partial shroud (PS) attached to the rotor blade tip at three values of tip clearance, viz. τ=2.2%, 6.1% and 7.9% of rotor blade height at the exit. The rotor exit flow is measured using a precalibrated five hole probe at three flow coefficients, namely, ϕ=0.18 (below design flow coefficient), ϕ=0.28 (design flow coefficient) and ϕ=0.34 (above design flow coefficient). The axial distribution of total pressure coefficient at rotor exit for the three flow coefficients clearly indicate increase in total pressure in the rotor tip region for the configuration with PS compared to that for the basic configuration. Similar increase is observed in the static pressure distribution at the rotor exit for the higher values of clearance. The mass averaged total and static pressures at the rotor exit for both configurations at the three values of tip clearances clearly show that partial shrouds are beneficial in improving the pressure rise of the compressor. This benefit is found to be more at the higher value of tip clearance tested.***

Keywords: Centrifugal Compressor, Tip Clearance, Casing Static Pressure, Fast Response Pressure Transducer *compressor,* Tip Clearance, Casing, Impeller

1. Introduction

The centrifugal compressors have a wide range of applications especially for power plants for small aircraft and helicopters, in process industries, compression of gases and vapours, because they can provide high-pressure ratios and large operating ranges with relatively high efficiencies. Centrifugal compressors are used primarily for their suitability for handling small volume flows, but other advantages include a shorter length than an equivalent axial flow compressor, less susceptibility to loss of performance by buildup of deposits on the blade surfaces and their suitability to operate over a wide range of mass flow. The efficiency of a centrifugal compressor is lower than that of an axial flow compressor. Efficiency is probably the most important performance parameter for turbomachines. The conditions of flow in the tip region of rotor blades are very complex, due to strong interaction of the leakage flow with the boundary layers and secondary flows. The tip leakage flow thus would have dominant effect on the performance of a compressor. A comprehensive review of tip clearance effects in centrifugal compressors is given by Pampreen (1983). Senoo and Ishida (1987) gave analytical expression to quantify the tip clearance effects in centrifugal blowers. Senoo (1991) gave a comprehensive review of mechanics of tip leakage flows in axial and centrifugal compressors. Ishida et al. (1987) had tested centrifugal blowers with different shapes (square, round and E-type, i.e. with an extension on the pressure surface side) and found that E-type tip provided improved performance. Sitaram and Swamy (2011) had tested a centrifugal compressor with different types of passive means, viz. turbulence generator at different positions and partial shroud attached the rotor blade tip and found that the partial shroud gave improved performance at all the values of the tip clearance. Hence the present investigation is undertaken to further explore the reason for this improvements. The paper reports these measurements at three flow coefficients, namely ϕ=0.18 (below design flow coefficient), ϕ=0.28 (design flow coefficient) and ϕ=0.34 (above design flow coefficient).

2. Experimental Facility, Partial Shroud and Instrumentation

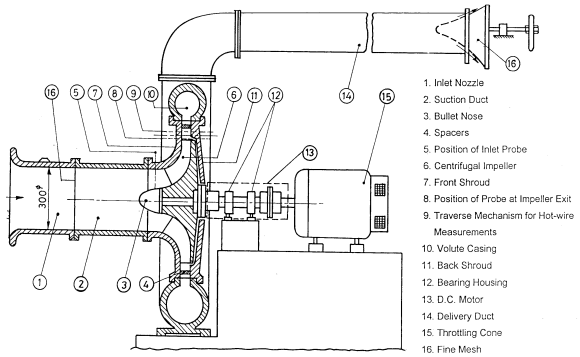

Figure 1: Schematic diagram of centrifugal compressor setup

Table 1: Design Details of the Rotor

Total pressure rise, Δp:	300 mm WG
Volume flow rate, V:	1.12 m^3/s
Speed of rotation, N:	2000 rpm
Shape number, N_{sh}:	0.092
No. of rotor blades, Z:	16
Inducer hub diameter, d_{1h}:	160 mm
Inducer tip diameter, d_{1t}:	300 mm
Rotor tip diameter, d_2:	500 mm
Blade height at the exit, h_2:	34.74 mm
Blade angle at inducer tip, β_{1t}:	35°
Blade angle inducer hub, β_{1h}:	53°
Blade angle at exit, β_2: (a) At hub:75°, (b) At mean section:90°, (c) At tip: 105°	
All the angles are measured w. r. t. tangential direction	

Experimental Facility: The present experimental investigations are carried on a low speed centrifugal compressor set up available in Thermal Turbomachines Laboratory, Department of Mechanical Engineering, Indian Institute of Technology Madras. A schematic layout of the experimental set up is shown in Fig. 1. The experimental set up consists of essentially a centrifugal rotor driven by a 5 kW D.C. motor with a rated speed of 2000 rpm. The D.C. motor is directly coupled to the shaft carrying the rotor. The main components of the compressor are suction duct, rotor, vaneless diffuser formed by the front and rear walls of the casing and volute casing of circular cross section and a delivery duct with a throttle at its outlet and nozzle at the inlet.

The major design details of the compressor are given in Table 1.

Partial Shroud: The partial shrouds are made of stainless steel of 0.1 mm thickness. The stainless steel sheet is cut to the shape of rectangle pieces of 50 mm x 5 mm size. These rectangle pieces are attached to the tip of the blades using araldite. The configurations tested (basic configuration without partial shroud and configuration with partial shroud) are shown in Fig. 2. The blade-to-blade view showing the partial shroud on the rotor tip is also shown in Fig. 2.

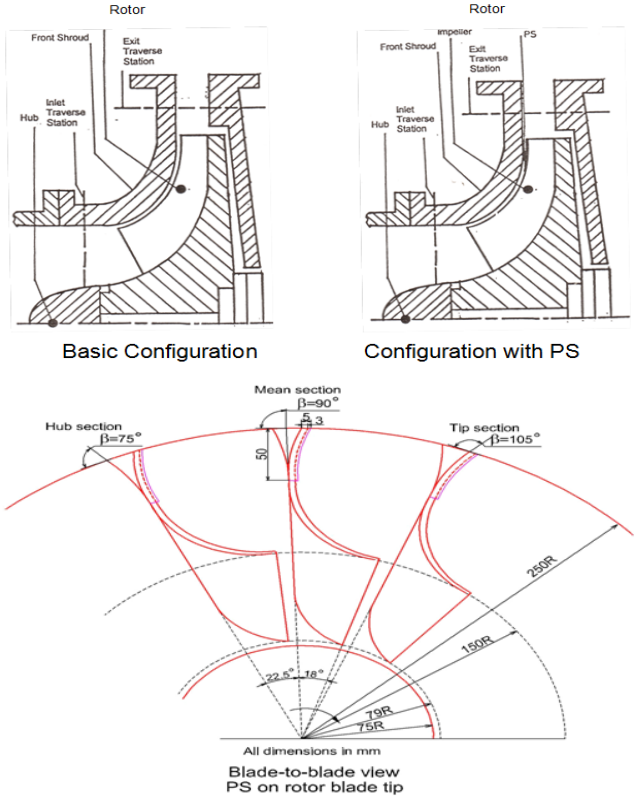

Blade-to-blade view with PS on the rotor tip

Figure 2: Details of Configurations Tested

2.1 Instrumentation

The performance of the compressor is determined by the change in the static pressure across the compressor. The static pressures on the suction duct and delivery duct are measured using a scanning box (Model FC091-3) and micromanometer (model FCO12) manufactured by M/s Furness Control Ltd. The scanning box contained 20 valves, which are numbered sequentially. The pressures to be measured are connected to the numbered inputs. Pressure inputs are read in sequence by using the micromanometer. The micromanometer is a sensitive differential pressure measuring unit, capable of reading air pressures from 0.01 mm to 2000 mm WG. It would respond to pressure inputs upto 50 Hz. But the time constant potentiometer can be used to average the pressure fluctuations.

The speed of the centrifugal compressor is measured using a non-contact type digital tachometer. Four interconnected static pressure tappings on the inlet bell mouth casing wall at the throat section are used to determine the inlet velocity. Knowing the bellmouth area, the volume flow is calculated using a suitable value of coefficient of discharge for the bellmouth. A D.C. motor with a separate exciter drives the centrifugal compressor. The input power was measured by mean of voltmeters and ammeters connected separately for field and armature supplies. A suitable value of motor efficiency is used to get the rotor input power.

The static pressure on the diffuser is measured at the above tip clearance at three flow coefficients, viz. ϕ=0.18 (below design flow coefficient), ϕ=0.28 (design flow coefficient) and ϕ=0.34 (above design flow coefficient). A precalibrated five hole probe is used to measure the rotor exit flow at the three values of tip clearance and at the above three values of flow coefficient. The probe is calibrated at two velocities to estimate the effect of Reynolds number on the calibration and the effect is found to be small. The non-nulling method of Treaster and Yocum (1979) is used.

3. Results and Discussion

Performance Characteristics: The results of the present investigation are presented and discussed in this section. The performance of the compressor in terms of ψ vs. ϕ and η vs. ϕ are presented. The non-dimensional parameters are defined as follows:

Flow coefficient, $\phi = \dfrac{V}{\pi d_2 b_2 U_2} = \dfrac{c_{2r}}{U_2}$

where
V=Volume flow (m^3/s)
d_2=Rotor tip diameter (m)
b_2=Rotor blade width at exit (m)
c_{2r}=Radial velocity at rotor exit (m/s)
U_2=Rotor tip speed (m/s)

Energy coefficient, $\psi = \dfrac{2W}{U_2^2}$

where
W=Specific work (m^2/s^2)
$= \dfrac{p_d - p_s}{\rho} + \dfrac{c_d^2 - c_s^2}{2} + g\Delta Z$

Power coefficient, $\gamma = \dfrac{2N_c}{\rho A U_2^3} = \dfrac{2\eta_m EI}{\rho A U_2^3}$

where
N_c = Coupling power (Watts)
A = Suction duct area (m^2)
E = Motor voltage (Volts)

I = Motor current (Amps)
η_m = Motor efficiency

Compressor efficiency, $\eta = \frac{\rho V W}{N_C}$

Figure 3 shows the performance characteristic in terms of energy coefficient, ψ vs. flow coefficient, ϕ for the three values of tip clearance for both configurations. At all values of tip clearance, PS gives higher value of energy coefficient, as the partial shroud obstructs the tip leakage flow and allows it to mix with main flow at a further distance. It may be observed that the performance of the rotor without PS at τ=2.2% is almost similar to that the rotor with PS at τ=5.1%. Hence by using partial shroud the rotor can operate at higher clearances with mechanical safe margins but without sacrificing performance.

Figure 4 shows the performance characteristic in terms of efficiency, η vs. flow coefficient, ϕ for the three values of tip clearance for both configurations. At all values of tip clearance, PS gives higher value of efficiency compared to that without PS due to reduced tip leakage flows. In fact the efficiency of the rotor with PS even at the highest value of tip clearance tested is higher than the efficiency of the rotor without partial shroud at the lowest value of tip clearance.

The most important performance parameters showing the effect of PS are presented in Table 2. It can be concluded that partial shroud is very beneficial to the performance of the compressor. The possible reason for the improvement in the compressor performance due to this small extension reducing tip leakage flows. It must be emphasized here that the performance presented above includes not only losses in the rotor, but also losses in the diffuser, volute and downstream duct with 90° bends.

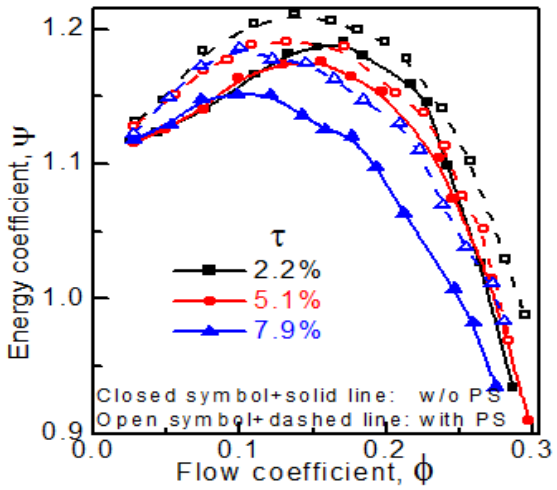

Figure 3: Performance of the centrifugal compressor: ψ vs. ϕ curve

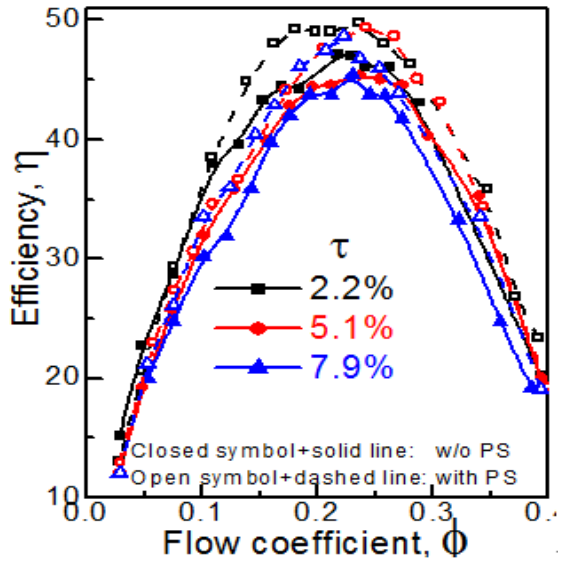

Figure 4: Performance of the centrifugal compressor: η vs. ϕ curve

Table 2: Effect of tip clearance on ψ_{max} and η_{max}

Details of Configuration	τ (%)	ψ_{max}	ϕ at ψ_{max}	η at ψ_{max}	η_{max}	ϕ at η_{max}
Without PS	2.2	1.188	0.169	44.5	47.1	0.217
	6.1	1.173	0.156	39.9	45.4	0.237
	7.9	1.153	0.121	31.9	45.5	0.230
With PS	2.2	1.204	0.139	44.8	49.7	0.237
	6.1	1.186	0.109	36.6	49.4	0.241
	7.9	1.185	0.101	33.5	48.6	0.222

Static pressure on casing: The static pressure distribution on the casing for the three values of tip clearance at three flow coefficients for both configurations is shown in Fig. 5. On the casing, 8 nos. of static pressure taps are provided from the inducer leading edge to the rotor exit. The locations of the taps are shown as inset in Fig. 3. The casing has its inner contour shaped to match the rotor blade tip from the inlet to the exit of the rotor. The static pressure measurements on the casing give an indication of variation of the static pressure developed in the tip region of the rotor. The static pressure coefficient is defined as follows:

$$\square_{Ws} = 2P_W / \rho U_2^2$$

From the figure it can be seen that the static pressure distribution is high for lower tip clearance when compared that at the higher tip clearance for all the flow coefficients. For the high flow coefficient considered, reduction in static pressure is higher near the inducer when compared to that at low flow coefficient. The pressure initially decreases due to suction and then uniformly increases, indicating that there is no dead zone or eddies near the casing region inside rotor and of the energy is transferred smoothly to the fluid near the casing.

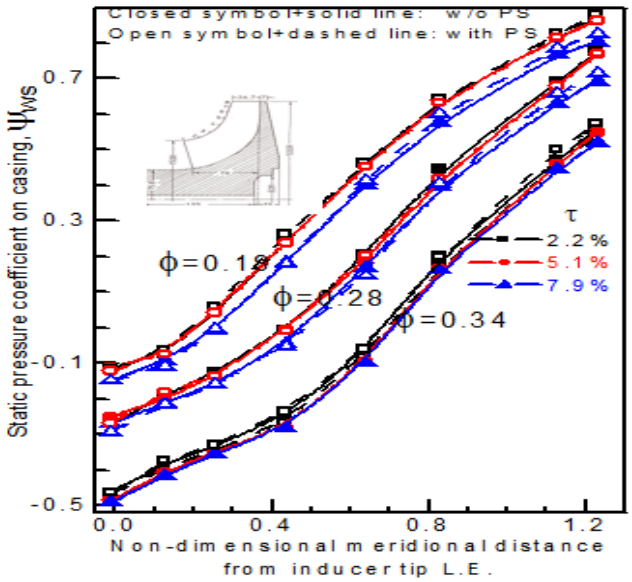

Figure 5: Distribution of static pressure on the casing

Table 3: Meridional view of impeller showing static pressure measurement positions

S.NO.	1	2	3	0	5	6	7	8
$\frac{m}{m_o}$	-0.13	0.00	0.10	0.26	0.40	0.67	0.88	1.00

3.1. Rotor Exit Flow Measurements

Total Pressure Coefficient, ψ_o: The distribution of total pressure coefficient at the rotor exit for both configurations and three flow coefficients at the three values of tip clearances is shown in Fig. 6. The total pressure coefficient is defined as follows:

$$\psi_O = 2P_o / \rho U_2^2$$

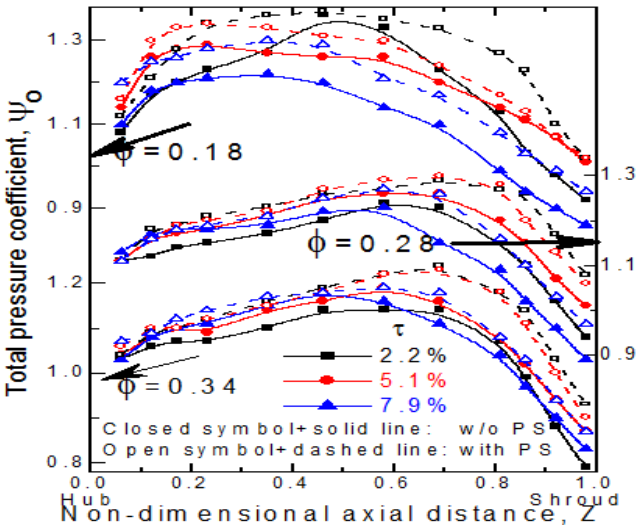

Figure 6: Distribution of total pressure coefficient at the rotor exit (For legend see Fig. 5)

From the figure, it can be clearly seen that rotor with partial shroud (PS) shows increased total pressure coefficient, (ψ_o) compared to basic configuration for all the flow coefficients at the tip clearance (τ=2.2%). From the figure, it can be seen that the extent of region of improvement increases with reduction in flow coefficient. That means the higher the loading more is the benefit due to the partial shroud. For the tip clearance τ=5.1%, the benefits of PS are reduced. It can also be observed that, the total pressure coefficient increases as the flow coefficient decreases for all the tip clearances. For tip clearance τ=7.9% configuration with partial shroud also shows higher total pressure coefficient compared to basic configuration. This may be attributed to the partial shrouds attached to the tip of the blades restricting the tip leakage flow and hence increased total pressure is obtained. Trend of the total pressure coefficient is almost same for both configurations at three values of tip clearances.

Static Pressure Coefficient, ψ_s: The static pressure coefficient distribution at the rotor exit for two configurations and three flow coefficients for three values of tip clearances is shown in Fig. 7. The static pressure coefficient is defined as follows:

$$\psi_s = 2P_s / \rho U_2^2$$

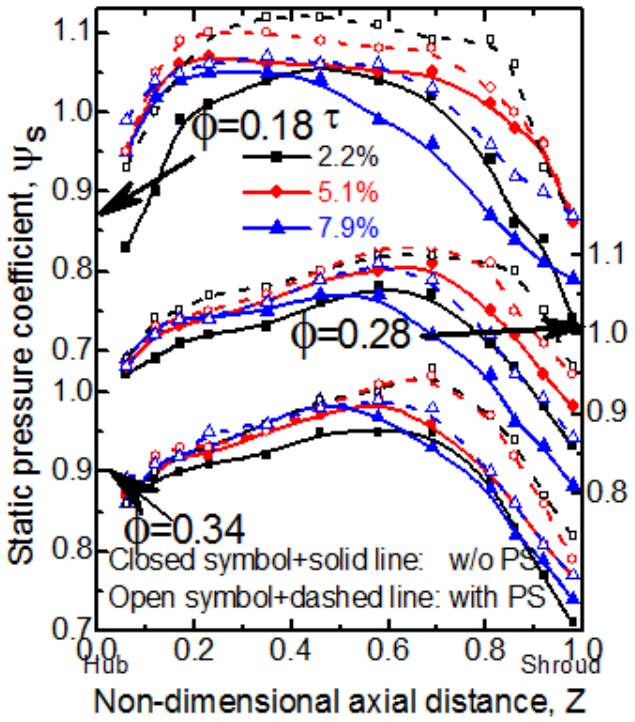

Figure 7: Distribution of static pressure coefficient at the rotor exit

From the figure, it can be clearly seen that rotor with partial shroud (PS) shows increased static pressure coefficient, (ψ_s) compared to basic configuration for all the flow coefficients at the three values of tip clearances (τ=2.2%, 5.1% and 7.9%). Similar to total pressure distribution, PS improves static pressure for a larger extent from the shroud, as the flow coefficient decreases. It can also be observed that, the static pressure coefficient is increasing as the flow coefficient increases for all the tip clearances. This may be attributed to the partial shrouds attached to the tip of the blades restricting the tip leakage flow. Trend of the static pressure coefficient is almost same for both configurations at three values of tip clearances.

Absolute Velocity, c: The axial distribution of non-dimensional absolute velocity at the rotor exit for two configurations and three flow coefficients for three values of tip clearances is shown in Fig. 8. Velocity and its radial and tangential components are non-dimensionalized with the rotor tip speed. From the figure, it can be seen that the absolute velocity increases with flow coefficient for all the tip clearances. For the three values of tip clearances at two flow coefficients (ϕ=0.34 and 0.28) clearly indicates an increase in absolute velocity in the rotor shroud region for the configuration with partial shroud, compared to the basic configuration. This is due to increase in tangential velocity, which means increased energy transfer. At flow coefficient (ϕ=0.34) an increase in absolute velocity is seen in the rotor hub region for the configuration with partial shroud, compared to the basic configuration. Trend of the absolute velocity is almost same for both configurations at three values of tip clearances. A careful study of this figure shows that basic configuration give lower absolute velocity for all the flow coefficients and for the three values of tip clearances. This lower absolute velocity is due to leakage flow in the flow field, which mixes with the main flow at the exit, resulting in lower values of velocities.

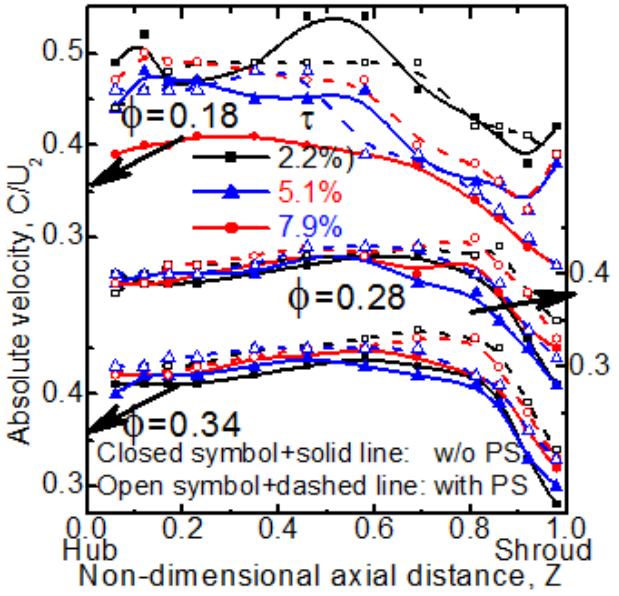

Figure 8: Distribution of non-dimensional absolute velocity at the rotor exit

Radial Velocity, c_r: The distribution of non-dimensional radial velocity at the rotor exit for three flow coefficients and two rotor configurations for three values of tip clearances is shown in Fig. 9. For three values of tip clearances, it can seen that radial velocity increased at flow coefficients (ϕ=0.34 and 0.28) in the rotor shroud region for the configuration with partial shroud, compared to the basic configuration. It can be observed from the figures that at the shroud region for three values of flow coefficients show decrease in radial velocity for hub region. At shroud region, boundary layer thickness increases due to partial shroud. Therefore higher loading on the blade causes decrease in radial velocity in the hub region.

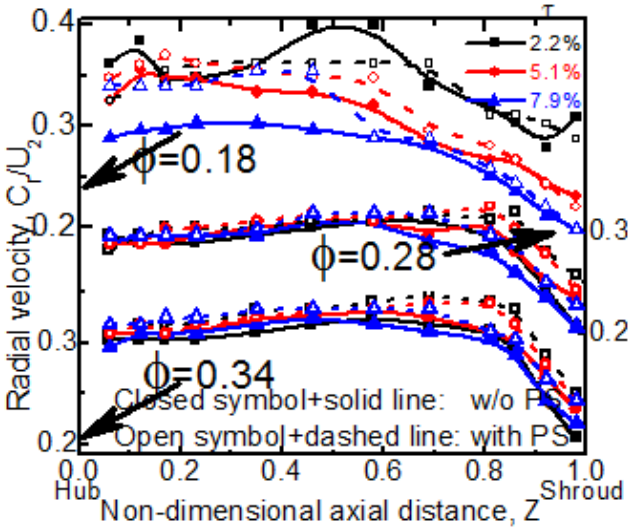

Figure 9: Distribution of non-dimensional radial velocity at the rotor exit

Tangential Velocity, c_u: The axial distribution of non-dimensional tangential velocity for the three flow coefficients and for both configurations, and for three values of tip clearances at the rotor exit is shown in Fig. 10. From the figure, it can be clearly shown that configuration with partial shroud increases tangential velocity for two flow coefficients (ϕ=0.34 and 0.28) compared to the basic configuration of rotor. But at flow coefficient (ϕ=0.18), configuration with partial shroud shows increased tangential velocity for hub region. Also the trend of tangential velocity is almost same for both configurations at the three values of flow coefficients.

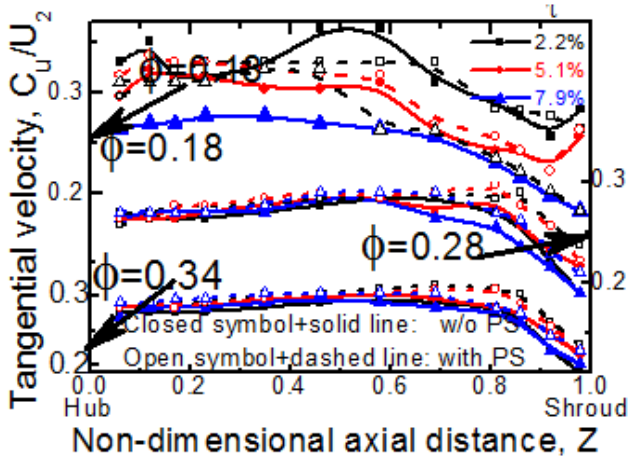

Figure 10: Distribution of non-dimensional tangential velocity at the rotor exit

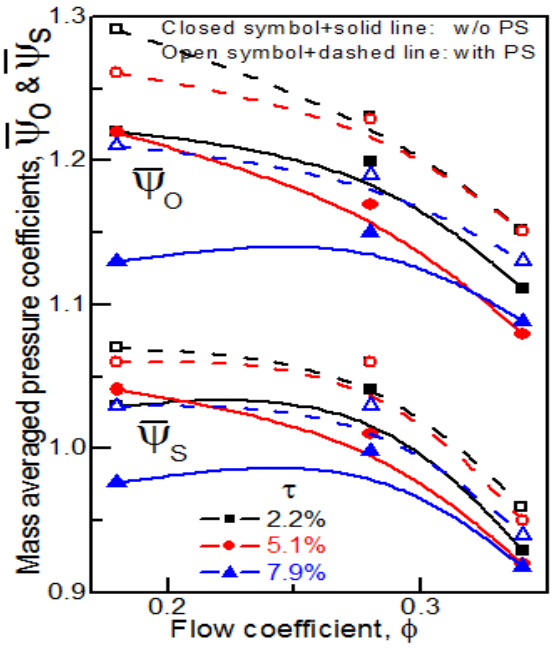

Figure 11: Mass averaged performance of the rotor

Mass Averaged Performance of the Compressor: Mass averaged performance of compressor (Fig. 11) shows the variation of mass averaged values of total pressure coefficient ($\bar{\psi}_O$) and static pressure coefficient ($\bar{\psi}_S$) with flow coefficient. The mass averaged values are defined as follows:

$$\bar{\psi}_O = \int_h^s \psi_O c_r dx / \int_h^s c_r dx \;\&\; \bar{\psi}_S = \int_h^s \psi_S c_r dx / \int_h^s c_r dx$$

The mass averaged values of total pressure coefficient ($\bar{\psi}_O$) and static pressure coefficient ($\bar{\psi}_S$) at the rotor exit for both configurations at the three values of tip clearances clearly show that partial shrouds are beneficial in improving the pressure rise of the compressor, compared to the basic configuration. It can also be observed that, the mass averaged values of total pressure coefficient ($\bar{\psi}_O$) and static pressure coefficient ($\bar{\psi}_S$) at the rotor exit for both configurations at the three values of tip clearances, increasing as the flow coefficient decreases. Also mass averaged values decrease with increase in tip clearance. From the figure, partial shrouds are found to have more beneficial effects at higher values of tip clearance.

4. Conclusions

The following major conclusions are drawn from the present investigation.

1. Configurations with partial shroud (PS) shows higher energy coefficient and efficiency compared to the basic configuration at all the values of tip clearance.
2. Basic configuration at τ=7.9% gives poor performance i.e. reduced operating range, reduced energy coefficient and efficiency over the entire operating range. Partial shrouds have beneficial effects in increasing energy coefficient and efficiency of compressor.
3. For three values of tip clearances, it can seen that radial velocity increased at flow coefficients (ϕ=0.34 and 0.28) in the rotor shroud region for the configuration with partial shroud, compared to the basic configuration. Radial velocity at the exit of rotor almost remains constant from hub to shroud for all the configurations and flow coefficients. (τ=2.2%, 6.1% and 7.9% &, ϕ=0.18, ϕ=0.28, ϕ=0.34 coefficient).
4. The tangential velocity at rotor exit decreases with increase in flow coefficient and this difference is reduced with decreasing flow coefficient. Partial shroud increases tangential velocity for two flow coefficients (ϕ=0.34 and 0.28) compared to the basic configuration of rotor. But at flow coefficient (ϕ=0.18), configuration with partial shroud shows increased tangential velocity for hub region.
5. The mass averaged total pressure coefficient and static pressure coefficients are higher for configuration with partial shroud (PS) compared to basic configuration. The possible reason may be due to reduction in the detrimental effects of the tip clearance flows by the partial shroud. Partial shrouds have more beneficial effects at higher values of tip clearance.
6. As the tip clearance is increased, there is a reduction in static pressure rise across the compressor, which causes reduction in energy coefficient. The decrease in energy coefficient is more at higher value of flow coefficient. The operating range slightly decreases with the increase in tip clearance.
7. The wall static pressure is high for lower tip clearance for all the flow coefficients. For high flow coefficient, reduction in static pressure is more near the inducer, which indicates more deceleration of flow at higher flow coefficient. The tip clearance is more pronounced at higher flow coefficients. From the graphs it shows that the maximum pressure is achieved for 2.2% tip clearance, as compared to other tip clearance, for all flow coefficients. Similarly for a flow coefficient of 0.28, the static pressure observed is higher than other flow coefficients for all tip clearances.

5. Nomenclature

b	Distance between the shroud and hub at the rotor exit (m)
C_d	Velocity in delivery duct (m/s)
C_s	Velocity in suction duct (m/s)
d	Rotor diameter (m)
N	Rotational speed of rotor (rpm)
N_c	Coupling power (Watt)
N_{sh}	Shape number = $N\sqrt{V}/W^{3/4}$
P_S	Static pressure (Pa)
P_O	Total pressure (Pa)
p_d	Delivery pressure (Pa)
p_s	Suction pressure (Pa)
t	Clearance of the rotor blade (m)
U_2	Rotor tip speed = ($\pi d_2 N/60$) (m/s)
V	Volume flow rate (m^3/s)
W	Specific work (m^2/s^2)
ϕ	Flow coefficient (defined in the text)
γ	Power coefficient
η	Efficiency (defined in the text)
ψ	Energy coefficient (defined in the text)
ψ_o	Total pressure coefficient= $2P_O/U_2^2$
ψ_s	Static pressure coefficient= $2P_S/U_2^2$
ρ	Density of air (kg/m^3)

τ	Relative tip clearance = (t/b_2)
Superscript	
-	Mass averaged value
Subscript	
2	Tip

6. Acknowledgements

The authors would like to thank the faculty, technical staff and administrative staff of Thermal Turbomachines Laboratory for their help and encouragement during the course of the present investigation.

References

[1] Ishida, M. and Y. Senoo, (1981) On the Pressure Losses due to the Tip Clearance of Centrifugal Blowers, Trans. ASME J. of Engg. for Power, 103(2) 271-278.
[2] Ishida, M., Ueki, H. and Senoo, Y., 1990, "Effect of blade tip configuration on tip clearance loss of a centrifugal blower", ASME J. Turbo., 112(1) 14-18.
[3] Pampreen, R. C., (1983) "Small Turbomachinery Compressor and Fan Aerodynamics", ASME J. of Engg. for Power, 105(2), 251-256.
[4] Schumann, L. F., Clark, D. A. and Wood, J. R. (1987) "Effect of Area Ratio on the Performance of a 5.5:1 Pressure Ratio Centrifugal Impeller", ASME J. of Turbo., 109(1) 10-19.
[5] Senoo, Y., (1991) "Mechanics on the Tip Clearance Loss of Impeller Blades", ASME J. of Turbo., 113 (3), 581-597.
[6] Senoo, Y. and Ishida, M. (1987) "Deterioration of Compressor Performance due to Tip Clearance of Centrifugal Impellers", ASME J. of Turbo., 109 (1), 55-61.
[7] Sitaram, N. and Pandey, B. (1990) "Tip Clearance Effects on a Centrifugal Compressor", J. of the Aero. Society of India, 42 (2) 309-315.
[8] Sitaram, N. and Swamy, S. M. (2011) "Performance Improvement of a Centrifugal Compressor by Passive Means", paper accepted for presentation at the 38th NCFMFP and publication in the proceedings.
[9] Treaster, A. L. and Yocum, A. M. (1979) "The calibration and application of five-hole probes", Trans. of ISA, 18(3), 23-34.
[10] M. Schleer and R. S. Abhari, "Clearance Effects on the Evolution of the flow in the vaneless diffuser of a centrifugal compressor at part load condition," ASME Journal of Turbomachinery, Vol. 130, 2008, pp. 1-9.
[11] D. Eckardt, "Detailed Flow Investigations within a High Speed Centrifugal Compressor Impeller," ASME Journal of Fluids Engineering, Vol. 98, No. 3, 1976, pp. 390-402. doi:10.1115/1.3448334.
[12] M. Inoue and N. A. Cumpsty, "Experimental Study of Centrifugal Impeller Discharge Flow in Vaneless and Vaned Diffusers," ASME Journal of Engineering Gas Turbines Power, Vol. 106, No. 2, 1984, pp. 455-467. doi:10.1115/1.3239588.
[13] Eum,Hark:Jin,Kang,Shin:Hyoung,Numerical study on tip clearance effect on performance of a centrifugal compressor,Proceedingsofthe2002 ASMEJointU.S.:European Fluids Engineering Conference,Montreal,USA,Jul 14-18 2002.